

# Segmentation of 3D nano-scale polystyrene balls

OLENA TANKYEVYCH<sup>1</sup>, LASZLO MARAK<sup>\*,1</sup>,  
HUGUES TALBOT<sup>1</sup> and PETR DOKLADAL<sup>2</sup>

<sup>1</sup> Institut Gaspard-Monge,  
Laboratoire A2SI, Groupe ESIEE, Noisy-le-Grand, France  
{tankyevo, talboth}@esiee.fr

<sup>2</sup> CMM, École des Mines de Paris, Fontainebleau, France  
petr.dokladal@cmm.ensmp.fr

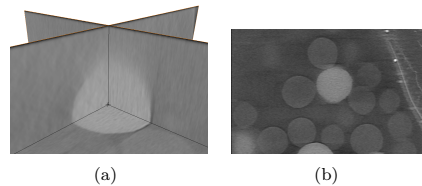


Figure 1. Sample image. (a) Cross section of the fully (horizontal) and partly (vertical) reconstructed image planes. (b) Complete image plane.

## 1. Introduction

In this project, we were interested in segmenting 3D images of nano-scale precursors of polystyrene balls. These roughly spherical objects of size range 100–300 nm were nucleated around an existing silica ball. The aim was to find the size and location of all the polystyrene balls with respect to the silica one.

The work details a segmentation method of both polystyrene and silica balls from a nanotomographic incompletely reconstructed image.

## 2. Materials and methods

The material consisting of polystyrene and silica balls embedded in a substrate was imaged with a Transmission Electron Microscope (TEM) in nanotomographic mode. This modality is similar in principle to standard X-Ray tomography. There is a number of key differences, however. First, electrons are used instead of high-energy photons. Second, a full 2D attenuation pattern is recorded at each angle. Moreover, due to sample thickness constraints, a full 180 degree rotation of the sample is impossible, hence the image reconstruction is incomplete.

The studied 3D image was obtained by rotation of the material sample through 140 degrees and its electron attenuation pattern was recorded using a constant angular step. As a result, the image data are of high quality at the equator, but noisy at the poles. The difference between fully and partly reconstructed planes is shown in the Figure 1.

## 3. Segmentation methodology

As a preprocessing step, in order to reduce the noise produced during image reconstruction, several filtering methods were used: 3D mean filtering, 2D edge extraction, 3D connectivity filter as well as openings and closings.

\*ujoimro@gmail.com

In order to detect circles from 2D slices of the image volume, the Hough circle transform was used. The original Hough transform [4] and its derivatives have been largely applied and recognized as a robust technique [5].

In the current work, the 2D Hough circle transform was used in order to detect the circles on each fully reconstructed (horizontal) 2D slice. On such slices, insufficiently reconstructed ball poles appear very dim, while well-reconstructed ball slices near the equator appear well separated from the background. The method succeeded in localizing circle centres and radii even from incomplete initial circles. As a result, a number of arcs with one centre and different radii were produced per circle. Circles were reconstructed by means of the radii of all the arcs associated with one centre.

Since a circle centre is obtained for each ball on every slice where the method succeeded, in the 3D data all detected centres are vertically aligned. To locate the centre of each ball with a good approximation, we selected the centre with the largest radius.

The result of the Hough transform on the filtered 2D image is shown in the Figure 2.

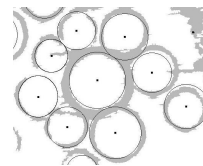


Figure 2. A pre-processed image slice together with the Hough circle transform result.

Since the Hough approach provided only an approximate centre  $C$  and radius  $R$  of a material ball, a segmentation improvement is desired.

In classical morphological segmentation terms [6] internal and external markers are required. A ball of radius  $0.7R$  centered in  $C$  was used as the internal marker. The complement of a ball of radius  $1.2R$  centered in  $C$  was used as the external marker. The intersection of all the external markers for all balls can also be used as a single external marker.

Due to the gradient's high sensitivity to noise, we used the modulus of a cubic spline-regularised discrete gradient [7].

A watershed segmentation [2] was used in the beginning of this projet, but due to the weak gradient this approach did not yield a good result. The final step of the segmentation was performed using the Continuous Maximal Flows (CMF) method [1]. In 3D, this approach globally minimizes the geodesic active surface equation [3] in the continuous domain by iteratively solving a system of linked Partial Differential Equations under linear constraints. The result is a continuous minimal cut (i.e. minimal surface) between the internal and external markers.

Initially, the minimal surface was computed over the metric given by  $g = \frac{1}{1+\|\nabla I\|}$ . However, in regions where  $g$  is near-constant (i.e. near the poles), the minimal surface is a portion of plane. To correct this defect, we used the known location of  $C$ . We weighted the metric by the inverse of the distance from this point, i.e.:  $g' = \frac{1}{r(1+\|\nabla I\|)}$ , with  $r$  the distance between the current point and  $C$ . Thanks to this weighting, the minimal surface is now a portion of a sphere centred on  $C$ , which is a-priori more consistent with the expected geometry of the material ball.

An example of an image of a polystyrene ball segmented by the CMF method is shown in Figure 3(a). Figure 3(b) shows the ball segmented without the metric weighting. We can observe an incorrect reconstruction due to weak gradient in this area of the image. A better segmentation result is shown in Figure 3(c). It was achieved using the  $1/r$  weighting described above.

#### 4. Conclusions and future work

We have suggested an acceptable segmentation procedure for 3D nanotomography images of polystyrene balls. It can still be improved. The CMF method is quite slow compared with watershed, we plan to use a multi-resolution approach to speed up calculations. A statistical analysis of the dispersion of centres and radii around the silica seed, which is a desired end-result of this study, is also forthcoming.

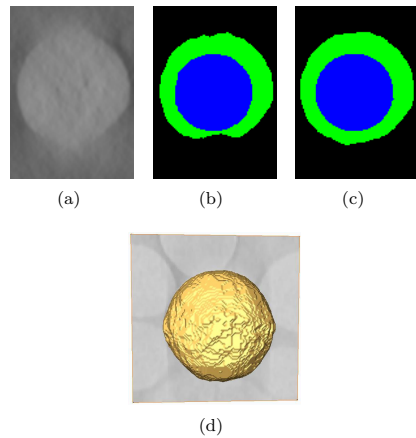


Figure 3. Slice of a segmented ball with the CMF method. (a) Original data. (b) Unweighted metric segmentation result in green (in blue - marker). (c) Weighted metric result (same color coding as in (b)). (d) 3D segmentation result.

#### Acknowledgements

The authors would like to thank Jean-Christophe Taveau, Olivier Lambert (IECB, Université Bordeaux1) and Etienne Duguet (ICMCB, Université Bordeaux1) for the images of polystyrene.

#### Bibliography

- [1] B. Appleton and H. Talbot, *Globally minimal surfaces by continuous maximal flows.*, IEEE Trans. Pattern Anal. Mach. Intell. **28** (2006), no. 1, 106–118.
- [2] S. Beucher and C. Lantuéjoul, *Use of watershed in contour detection*, Int. workshop on image processing, 1979Sept.
- [3] V. Caselles, R. Kimmel, and G. Sapiro, *Geodesic active contours*, International Journal of Computer Vision **22** (1997), no. 1, 61–79.
- [4] P. V. C. Hough, *Methods and means for recognizing complex patterns*, 1962.
- [5] J. Illingworth and J. Kittler, *A survey of the hough transform*, Comput. Vision Graph. Image Process. **44** (1988), no. 1, 87–116. Important reference.
- [6] F. Meyer and S. Beucher, *Morphological segmentation*, Journal of Visual Communication and Image Representation **1** (September 1990), no. 1, 21–46.
- [7] M. Unser, A. Aldroubi, and M. Eden, *B-spline signal processing, part ii: efficient design and applications*, IEEE Trans. Signal Processing **41** (1993February), 834–848.